CAL-2294

National Aeronautics and Space Administration

FINAL TECHNICAL REPORT

FOR NASA GRANT NAG 5-2593

Submitted by: The Trustees of Columbia University
in the City of New York
Box 20, Low Memorial Library
New York, New York 10027

Prepared by: Columbia Astrophysics Laboratory
Departments of Astronomy and Physics
Columbia University
538 West 120th Street
New York, New York 10027

Title of Research: "Large-Format High Resolution Microchannel Plate Detectors for Ultraviolet Astronomy"

Principal Investigator: Christopher Martin

Project Termination Date: 31 December 1994

March 1995

FINAL TECHNICAL REPORT FOR NAGW-2593

31 March 1995

The following summarizes the detector development work under the award entitled "Large-Format, High Resolution, Microchannel Plate Detectors for Ultraviolet Astronomy."

This report includes work on two types of two-dimensional position-sensitive detectors that were developed in this lab under this award. We worked to develop and optimize the wire-wound Helical Delay Line detector (HDL) in the first and second years. Some early work on the HDL is contained in a paper included as Appendix A. In the second and third years we developed the concept for, then successfully designed and tested, both a lab prototype, and a flight prototype of the first, crossed delay line detector based on two orthogonal Serpentine Delay Lines (SDL). Some of the work on the SDL is contained in a paper included here as Appendix B. A more extensive paper on the SDL work has been submitted to the Review of Scientific Instruments. Appendix C contains copies of the Invention Report to the Columbia University Office of Science and Technology Development. Also included in Appendix X is the response from that office declining to pursue a patent.

We are currently preparing to test fly four SDL detectors, the design for which was developed under this grant, in a sounding rocket launch from Australia, in October 1995, to map 1/4 of the sky in two narrow bands (CIV 1550Å and molecular hydrogen fluorescence) and two continuum bands, all in the far ultraviolet. This detector was also baselined in the definition study for the JUNO Small Explorer Mission.

Year 1

Improved preamp performance by rebuilding the front-end electronics using well-matched off-the-shelf preamps and other components assembled with appropriate radio-frequency techniques. All electronics are now out of vacuum so that the changes and tests can be made quickly. Replaced contaminated 50-mm MCP stack with 40-mm MCP stack. Discovered that the collecting wire must leave the anode on the inside at both ends of the anode for the signals to match for improved cancellation of charge-cloud variances. Made appropriate change to prototype anode. Discovered that electron cloud variance can contribute ≈ 50 μm to position resolution budget, but can be reduced by closing the MCP anode gap. Scrubbed stack for the purpose of reducing local aging and testing the hypothesis that ion feedback in unscrubbed MCP stack causes degradation of spatial resolution. Preliminary results indicate significant improvement. Determined inexpensive method for anode fabrication with wire precision to 3 μm and intrinsic linearity of 1 μm due to wire placement. Brought up workstation and image analysis software. Connected eithernet between workstations and acquisition computer. Further developed acquisition and analysis software based on software.

Year 2

Developed concept for construction of SDL and built prototype. Developed process for using laser ablation machining to cut precision slits in anode, which is required to allow read out of orthogonal position information. Continued work to determine origin of resolution limits. Performed extensive work on the origin and analysis of spatial nonlinearities in this type of detector (both SDL and HDL) and explored methods of reducing these effects. Developed flight design of HDL anode and performed shake test to prove robustness for launch into space.

Year 3

Continued testing SDL detector for resolution, spatial nonlinearity, and high count rate performance. Improved designs for preamplifiers to read out the SDL signals. Improved control impedance match between delay line and anode by modifying delay line fabrication parameters. Developed models and performed extensive computer simulations of pulses traveling on delay lines of different designs. This work permits delay line parameters to be chosen for optimized performance under different design requirements. Built and tested flight prototype SDL detector.

APPENDIX A

Two-Dimensional Helical Delay-Line Readout of Large-Format Microchannel-Plate Detectors for Astronomy

Peter G. Friedman, Judith R. Fleischman, and Christopher Martin
Columbia Astrophysics Laboratory
Departments of Astronomy & Physics, Columbia University
538 West 120th Street, New York, NY 10027, USA

To appear in: *Proceedings of the* 10^{th} *International Colloquium on UV and X-Ray Spectroscopy of Astrophysical and Laboratory Plasmas*
3 – 5 February 1992, Berkeley, CA

COLUMBIA UNIVERSITY

DEPARTMENTS OF

PHYSICS and ASTRONOMY

NEW YORK, NEW YORK 10027

Columbia Astrophysics Laboratory Contribution Number 486

Two-Dimensional Helical Delay-Line Readout of Large-Format Microchannel-Plate Detectors for Astronomy

Peter G. Friedman[1], Judith R. Fleischman[2], and Christopher Martin[1]

[1] Department of Physics, Columbia University
[2] Department of Astronomy, Columbia University

ABSTRACT

We report progress on a new readout for microchannel-plate detectors for astronomical imaging and spectroscopy. The two-dimensional helical delay-line readout should provide a 5000×5000-pixel, 10-cm×10-cm detector. Spatial resolution (FWHM) achieved to date is ~30—40 μm. The spatial linearity residuals are 3—9 μm over 2—4 mm. We also discuss expansion of the charge cloud, ion feedback, and local aging. We are proposing this detector for a small-explorer-based far-UV all-sky survey and plan to use it on a rocket-borne far-UV survey of the interstellar medium.

1 INTRODUCTION

For over a decade microchannel-plate (MCP) detectors have been the standard for astrophysical observations in the ultraviolet band. However, the potential return from many future experiments will be fully realized only with large-format detectors that obtain the highest possible spatial resolution, linearity, and dynamic range.

We think that the two-dimensional helical delay-line MCP readout (Sobottka and Williams 1988, Friedman, Martin, and Rasmussen 1990, Williams, *et al.* 1991) is the best candidate for development of a large-format detector. It is relatively inexpensive, and should achieve resolution sufficient to make full use of MCP-pore size (~10 μm). In contrast to charge-division readouts, increasing the size of this detector, within limits, does not degrade, and may actually improve the absolute spatial resolution. The format and throughput rate can both be large. We expect that the detector will be robust in launch and space environments, and will make only modest demands on spacecraft power, volume, and weight.

1.1 Detector Goals and Applications

We are currently testing a 15-cm anode with 40-mm MCP's. Our ultimate goal is to construct a 10-cm diameter detector with 5000×5000 pixels of 20-μm FWHM resolution and $\sim 10^6 s^{-1}$ throughput rate. The prototype detector now has sufficient resolution to provide ~2000×2000 pixels across a 65-mm diameter. This meets the requirement for the small-explorer-based far-UV all-sky survey we are proposing.

The all-sky survey mission would perform three complementary surveys. First, a one-year all-sky survey to a limiting magnitude of ~18 in three wavelength bands: 140, 160, and 180 nm. Second, deep surveys of 10—20 selected fields to 21—22 mag in the three bands. Third, an objective spectroscopic survey to 18th mag over ~2% of the sky, with $\Delta\lambda$=0.3−2.0 nm. The spectroscopic survey will permit a detailed look at a smaller, but substantial and varied sample of objects, as well as providing important basic data for the interpretation of the photometric surveys. It will furnish detailed information about the temperature, gravity, continuum slope, redshift, ionization, metallicity, stellar populations, and extinction for hundreds to thousands of sources in each class.

Within the next two years we plan to prove the space worthiness of the delay-line readout by flying three detectors on a rocket-borne far-UV survey of the interstellar medium (ISM). The large format and high throughput of delay-line detectors make it possible in a single 5-min rocket flight to map one quarter of the sky in three bands. The bands, defined by broad- or narrow-band filters, will be 140−190-nm continuum emission, CIV emission, and H_2 fluorescence. These will be the first maps made in the latter two bands. The maps will yield information on the morphology and degree of isotropy of the diffuse far-UV background and ISM, and allow us to study the interrelationships of its molecular, cold atomic, and hot phases.

2 THEORY OF OPERATION

The two-dimensional helical delay-line readout technique employs a crossed pair of flattened-helical bifilar transmission lines. Each delay line independently gives the position in one spatial dimension. Each delay line consists of a pair of bare Cu wires, one of which is biased to collect electrons. The electron cloud from a MCP event falls over several turns of each transmission line. From that region pulses propagate to timing electronics at both ends of each transmission line. Differential-mode signal amplification minimizes noise pickup and $x-y$ crosstalk. The pulse arrival times at the ends of each delay line give the event position.

The delay-line readout achieves its results by requiring pulses to travel ~300 times as far as they would in a straight path across the anode. This reduces the effective propagation velocity of the pulse, thereby reducing by the same factor the spatial uncertainty derived from a timing measurement.

3 RESULTS

3.1 Spatial Resolution and Linearity

The pinhole-array image in Fig. 1a gives an indication of the detector's performance. We have also measured the spatial resolution and linearity by precisely positioning a single nominal 10-μm UV spot on the front MCP. The gain of the Z-stack MCP is ~1×10^8. Spatial linearity residuals are 3−9 μm rms over 2−4 mm. The FWHM resolution is 30 μm in one dimension (x, upper wire plane) and 40 μm in the other (y, lower plane), including the contribution of the UV spot. This is an improvement over the 60-μm FWHM resolution quoted in Friedman, Martin, and Rasmussen 1990. We believe that the earlier, poorer, resolution resulted from extracting large amounts of charge from the MCP at the positions of the UV spots during setup (sec. 3.4).

3.2 Charge-Cloud Variance

We have found that MCP pulse-to-pulse charge-cloud shape variances (as well as ion feedback—sec. 3.3), are largely responsible for the difference between actual and theoretical spatial resolution. The effect of such variances on the spatial resolution should increase with the time available for the charge cloud to spread out as it travels from the MCP to the anode. To test the hypothesis that charge-cloud-shape variances are a dominant contribution to degradation of spatial resolution in this, and possibly in charge-division devices, we reduced the MCP-to-anode travel time by 42%. (This also reduced by ~20% the rise time of the wave form from which the timing information is extracted. However, this could not explain improved resolution because the system is not noise limited.) The resolution improved by 25—30%, a quadrature improvement of 30—40 μm. This supports the above hypothesis.

3.3 Ion Feedback

The funnel shape in Fig. 1b shows that the resolution degrades with increasing pulse height. This is in contrast to the noise-limited case in which resolution improves with signal amplitude. The MCP's used thus far were not electron scrubbed (or burned in), a preconditioning process which removes adsorbed gas and stabilizes aging. We hypothesize that the cause of the funnel shape is ion feedback. This causes after-pulses, seen in anode wave forms, that overlap with the initial pulse before it reaches the end of the delay line. If the hypothesis is correct, scrubbing the plates should improve the resolution by up to a factor of two.

3.4 Local Fatigue of the MCP

We are studying local aging effects that are intrinsic to MCP's. We have discovered that in unscrubbed plates local aging can significantly degrade local spatial resolution and linearity. Fig. 2 shows a 40% decrease in local MCP gain, accompanied by a factor of 2.7 degradation of the local spatial resolution, during the extraction of 0.5 C/cm^2 from a 2000-μm^2 area of the rear MCP. Fig. 1c shows the resulting spatial nonlinearity in the region around two fatigued spots, probed by a pinhole array. Large nonlinearity is apparent. We expect these effects to be independent of readout method and to be substantially reduced in scrubbed MCP's. However, the effects require further study to permit acquisition of fields containing bright stars, with pore-limited resolution, even using a "long-life" scrubbed detector.

5 DISCUSSION

The detector resolution is still dominated by ion feedback and MCP charge-cloud variance, not by electronics. These contribute ~20 μm to the spatial resolution, but can be reduced by electron scrubbing and further closing the MCP-to-anode gap. A smaller gap is permissible because there is no evidence of undersampling nonlinearity, which would be caused if the charge cloud covered too few wires. Our experience with ion feedback and local MCP aging underscores the importance of electron scrubbing even for laboratory prototype detectors. Finally, the resolution is already sufficient for the small-explorer far-UV survey mission.

6 REFERENCES

Friedman, P.G., Martin, C., and Rasmussen, A. 1990, *SPIE Proc.*, **1344**, 183.
Sobottka, S. E. and Williams, M. B. 1988, *IEEE Trans. Nucl. Sci.*, **35**, 348.
Williams, M.B. *et al.* 1991, *Nucl. Instrum. Methods*, **A302**, 105.

This work supported by NASA grants NAGW-1887, NAGW-2593 and NAG-5-642.

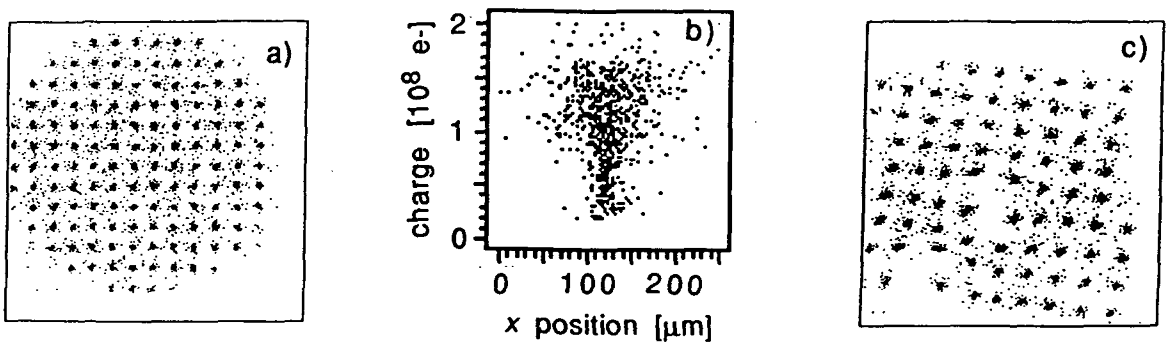

Fig. 1—a) Image of pinhole array with 10-μm pinholes on a 250 μm grid. b) Scatter plot of charge in event vs. measured position. c) Local linearity around fatigued area of MCP probed by pinhole array.

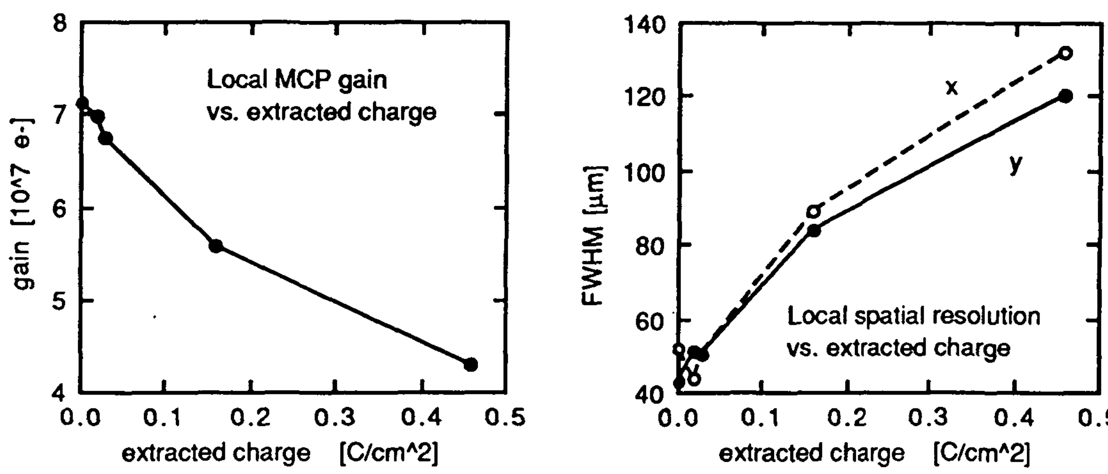

Fig. 2—Evolution of a small MCP region stimulated by a 10-μm UV spot. The plots show degradation in MCP gain and spatial resolution.

APPENDIX B

PROCEEDINGS REPRINT

SPIE—The International Society for Optical Engineering

Reprinted from

EUV, X-Ray, and Gamma-Ray Instrumentation for Astronomy IV

11–12 July 1993
San Diego, California

Volume 2006

Multilayer Anode with Orthogonal Serpentine Delay Lines for High Spatial Resolution Readout of Microchannel Plate Detectors

Peter G. Friedman, Raúl A. Cuza, Judith R. Fleischman, Christopher Martin, and David Schiminovich

Columbia Astrophysics Laboratory, Columbia University
538 West 120^{th} Street, New York, NY 10027

ABSTRACT

We have designed, built, and tested the first successful imaging microchannel-plate (MCP) detector that uses two orthogonal, printed circuit, serpentine delay lines in a three-dimensional architecture. Laser-ablation machining is used to cut slots that allow delay lines in two layers parallel to the MCP to sample and read out x and y image positions. Previous anodes that use delay-line timing to read out both dimensions of an image employ a wire-wound anode. The goal of this readout is to provide as many picture elements (pixels) as possible in two dimensions, with high temporal resolution, high throughput, high dynamic range, and good spatial linearity. This detector achieves this goal with off-the-shelf electronics and is robust for space flight. The full width half maximum (FWHM) spatial resolution is 32 μm at the center of the detector and is typically < 35 μm throughout the detector. The rms linearity is 40 μm in each readout dimension, after applying only radial corrections for fringe field effects near the perimeter, and < 20 μm after applying additional simple (1-dimensional) corrections. We discuss fabrication techniques.

1. Introduction

An attractive readout scheme for microchannel plates[1,2] that combines the advantages of a large format and high spatial resolution is the delay line anode. Reference 3 gives a more complete explanation of the work described here. The position in one dimension is determined by measuring the difference in arrival time of pulses propagating toward the ends of the delay lines from the anode location at which the MCP-generated electron cloud lands. A planar, microstrip version of such an anode can be realized using a so-called 'serpentine' delay line (SDL) which is constructed by conventional etching of copper-clad epoxy-fiber-glass or PTFE-ceramic composite printed-circuit boards. Lampton *et al.* [4] first showed experimentally that a single serpentine microstrip delay-line readout for a MCP detector could have high spatial resolution over a large, one-dimensional detector format ideal for spectroscopic detectors. In that work, one dimension is read out using the delay-line scheme and the other is read out using wedge-wedge charge division electrodes interleaved with the serpentine delay-line. The spectroscopic double delay-line (DDL), which uses two delay lines in one plane to read out the same dimension,[5] has achieved very high resolution (15 μm)[6] and a large format (90 mm) in one-dimension. Resolution in the perpendicular dimension can be almost as good ($\sim$30 μm) but the number of pixels and format are limited by the charge-division scheme, making the anode less suitable for imaging applications.

Siegmund *et al.*[7] has suggested the possibility of a multilayer serpentine delay-line anode that would extend large numbers of pixels into two dimensions. There is a geometrical reason that implementing this scheme is technically challenging. A delay line readout must sample the entire active area, but a single delay line can provide information about only one dimension. Two orthogonal delay lines are required in order to read out two dimensions. Since the delay line segments are perpendicular to the readout dimension, the

PRECEDING PAGE BLANK NOT FILMED

0-8194-1255-4/93/$6.00

delay lines must logically lie in different planes if they are not to interfere with each other. This multilayer scheme requires the electrons to pass through the plane of one delay line to reach the other delay line. Thus the architecture of the anode not only must be 3-dimensional, but must allow access to an interior layer at places throughout its surface area. It is this architecture that provides the technical challenge.

The work we present here is the first realization of the multilayer serpentine delay-line. Sobottka and Williams[8,9] have developed previoulsy a two-dimensional delay line anode constructed from orthogonal, bifilar, flattened helical transmission lines. In this design wires are wound on an insulating frame. The spaces between the wires in the upper plane allow the electrons to reach the lower plane. We have also constructed and characterized this helical delay line detector (HDL) in our laboratory.[10,11,12] The HDL has excellent resolution and linearity performance. However, concerns about the mechanical robustness of the suspended wires in the HDL for space applications, as well as some less-than-ideal electrical properties, led us to investigate a multilayer serpentine delay-line as part of a parallel effort in our laboratory. A detailed comparison of the SDL and HDL will be left to a future paper.[12]

Within the next year we plan to prove the space worthiness of the multilayer serpentine delay-line readout by flying four such detectors on a rocket-borne survey instrument designed to study far-UV emission from the interstellar medium.[13] The large format and high throughput of delay-line detectors make it possible to map nearly one quarter of the sky in three bands of the far ultraviolet in a single 300 s rocket flight.

2. Theory of operation

The SDL anode consists of two independent serpentine delay lines as shown in Fig. 1. Each delay line is a microstrip transmission line that is a printed circuit of bare copper on a dielectric substrate with a copper ground plane on the reverse side. One delay line reads out the x dimension, the other the y dimension. Fig. 1 shows an electron cloud leaving the bottom of the MCP stack. It lands on several adjacent segments of each delay line. Material is removed from between the segments of the delay-line closest to the MCP as shown on Fig. 2 to allow electrons to reach the lower delay line. From the region where the electrons fall onto the delay lines, voltage pulses propagate to timing electronics at both ends of each delay line. The difference of the pulse arrival times at the ends of each delay line contains the event position information in one dimension.

The delay-line readout achieves its resolution by combining high dielectric permittivity with a serpentine path to reduce the effective velocity of the pulses toward the timing electronics to a value much less than the speed of light. The effective velocity is given by $v_{\text{eff}} = fcp/l(\epsilon_r)^{1/2}$, where c is the speed of light, p is the full period pitch of the serpentine, l is the length of the serpentine strips, and ϵ_r is the relative permittivity. The value $f > 1$ is a fudge factor that accounts for divergences from an ideal microstrip circuit, including coupling between adjacent serpentine turns, inhomogeniety caused by slots in the dielectric, and coupling of both delay lines to the slotted upper ground plane. The x and y delay lines have different values of f. The difference of the arrival times of pulses at each end of one delay line is given by $t = t_2 - t_1 = [(l/2 + x)/v_{\text{eff}} - (l/2 - x)/v_{\text{eff}}]$, as shown in Fig. 1. The position is then calculated trivially to be $x = v_{\text{eff}}t/2$, completely independent of the orthogonal dimension. Since the start times decrease and the stop times increase at the same rate as the event position moves, the time difference changes at twice the rate.

This result generalizes to the y delay line with only a change in v_{eff}, which is due to differences in f. The anode was built with the values of l and p identical in both dimensions. The uncertainty in the position measurement in the x dimension is $\sigma_x = v_{\text{eff}}\sigma_t/2$, where σ_x and σ_t are the uncertainties in x and t, respectively, and similarly for the y dimension. Fixed timing errors in the electronics and voltage noise in the wave form contribute to σ_t as discussed in section 7.2. Thus lower values of v_{eff} reduce the spatial

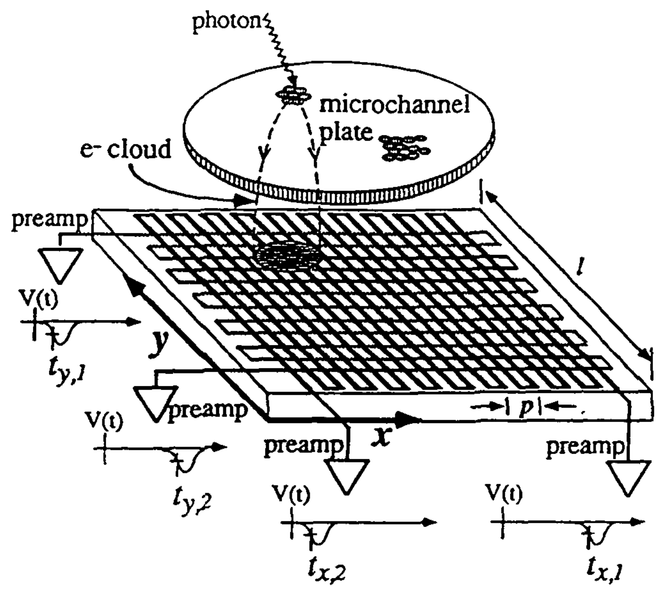

Fig. 1. Schematic of the theory of operation for the serpentine delay line readout, showing two independent delay lines lying in different planes. Each delay line is a serpentine, and the two delay lines are orthogonal. In each plane, a portion of the electron cloud from the microchannel plate stack produces two voltage pulses traveling toward the ends of that delay-line. The time difference between the pulses yields the event coordinate in one dimension. The orthogonal position is obtained from the time difference of pulses produced by MCP electrons falling on the other plane.

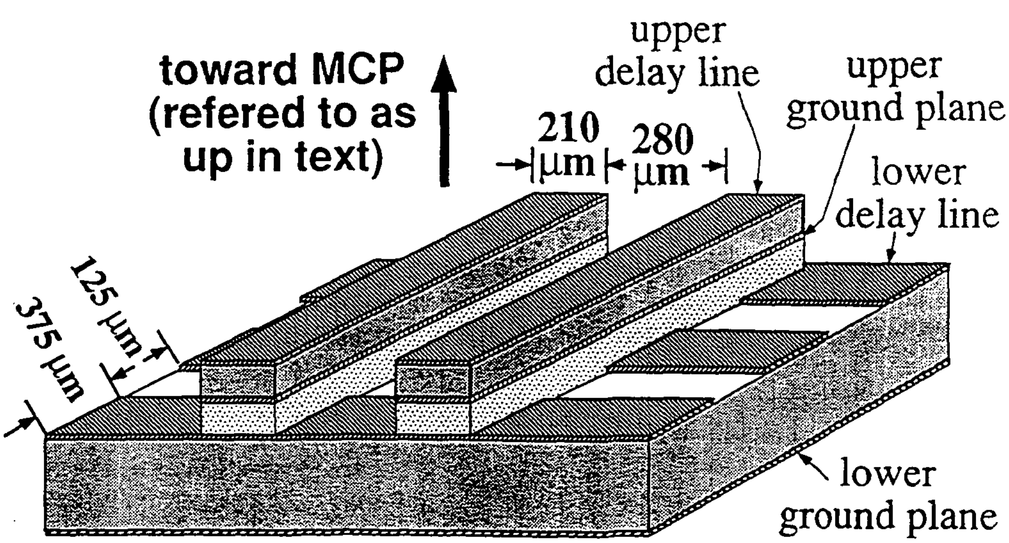

Fig. 2. Schematic showing cutaway detail of the 3-dimensional anode architecture. The figure shows upper and lower delay lines with their ground planes. Widths of strips and spaces are shown. Slots in the copper are etched before bonding. Dielectric is continuous during bonding of layers. Following bonding, slots in dielectric are cut by laser ablation. The copper acts as a reflective mask during laser ablation.

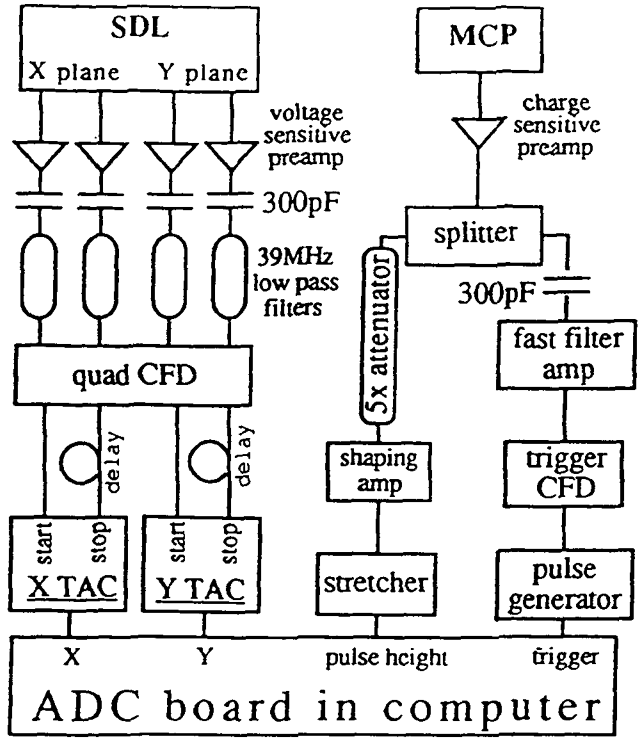

Fig. 3. Block diagram of readout electronics. The delay line preamps, which amplify the pulses leaving the delay-lines, are Phillips Scientific 6954. The 4-channel constant fraction discriminator (CFD), which provides amplitude-independent precise timing of the amplified pulses, is a Tennelec TC455. The time-to-amplitude convertors (TACs) convert start and stop pulses from the CFDs to a voltage are Ortec 457. The ADC converts the TAC voltage to a 12-bit digital number. We use a Data Translation DT2221-L ADC board operating in a Macintosh IIx computer.

uncertainty. For this anode, $cp/l(\epsilon_r)^{1/2} = c/640$ for both x and y. However, the measured velocity is more than two times faster due to the value of f.

3. Electronics

The function of the readout electronics shown in Fig. 3 is to extract and digitize two precise time differences, which are proportional to x and y, and a pulse amplitude and time for each MCP event. The electronics consist of standard voltage and charge-sensitive preamps and off-the-shelf frequency filters and NIM bin modules. Pulses propagate from the ends of the $\simeq$50 Ω delay lines into preamps with 50 Ω inputs. The preamp output is filtered by a 39 MHz (nominal) low-pass Bessel filter and a 300 pF series capacitor acting as a 10 MHz high pass filter. Constant fraction discriminators (CFDs), which find the time at which each wave form reaches 50% of its peak amplitude, extract the arrival time of each filtered pulse at each end of each delay line. These times, t_1 and t_2 in Fig. 1, are used respectively to start and stop a time-to-amplitude converter (TAC) for x and similarly for y. An additional delay on each TAC stop input insures that regardless of the event position on the MCP surface, the start signal from an event always preceeds the stop signal. The TAC output goes into an analog-to-digital converter (ADC) on a board in the acquisition computer.

In parallel with the delay line electronics, an independent channel of electronics extracts pulse amplitude and a trigger from a pulse induced on the electrode at the MCP output as the electrons leave the MCP.

The theory of operation and electronics are basically identical for the HDL and for the SDL.

4. Fabrication and Description

As explained in the section 1, the main technical hurdle to overcome in making this anode work is finding an architecture and fabrication method that permits half the electrons in a MCP event to travel through the plane of the upper delay line to reach the lower delay line. The design shown in Figs. 1 and 2 and the fabrication method described below solve this problem.[14] In particular, laser ablation machining makes possible truly three-dimensional architectures of the type we use.

One of the advantages of the serpentine delay-line anode is that the fabrication methods are commercially developed methods used for microstrip printed-circuit board fabrication. Fabrication of the anode begins with standard photolithography of two, double-sided, copper-clad, RT/duroid 6010 ceramic-filled PTFE dielectric ($\epsilon_r = 10.2$) boards[14a,15]. A .010 inch thick board is used for the upper delay line and a .025 inch board is used for the lower delay line. We define upper as closer to the MCP. On the upper side of each board, copper is etched away leaving only a single serpentine strip with solder pads at the end. The lower side of each board is the ground plane for the delay line that is on the upper side of that board. The ground plane for the lower delay line is solid. In addition, copper is removed from the upper ground plane in 80 mm long slots that line up precisely with the spaces between the segments of the upper delay line. The perimeter of the upper ground plane is continuous.

After the patterns have been etched, the boards are bonded to one another and to a brass substrate. The bonding is accomplished using a standard process for commercial fabrication of multilayer printed circuit boards called fusion bonding.[16] A material called bondply is stacked between the boards to be bonded. Bondply is a less dense, more porous form of RT/duroid 6002 ceramic-and-glass-filled PTFE dielectric. Heating bondply to 385°C under 1700 psi pressure changes it into RT/duroid 6002 material and causes it to fuse to adjacent materials that have appropriately treated surfaces. The bonding of the serpentine delay line anode takes place in two steps. The first step is to fuse bondply with a thickness of 60 μm to the brass plate at 1700 psi. The second step is a bond done at 250 psi. In this step the delay line boards are bonded to each other with 375 μm of bondply between them and the bottom delay line board is bonded with an additional piece of 60 μm-thick bondply to the bondply that was bonded to the back plate in the first step. The bondply between the delay line boards serves both to bond them together mechanically and as a dielectric ($\epsilon_r = 2.8$) space to decouple the delay lines electrically. The bonding is done in 2 steps because pressure above a few hundred psi causes the RT/duroid 6010 material to flow, but high pressure insures a good bond to the brass substrate.

After the anode has been bonded, material must be removed from between the segments of the upper delay line. The resulting slots extend down through the openings in the upper ground plane and expose the copper of the lower delay line. This allows about half of the electrons in a MCP event to pass through the upper delay line layer and reach the lower delay line. The slots are cut using laser ablation machining to remove dielectric material from the regions between the copper. A focused laser is rastered over the entire anode to remove any dielectric that is not masked by the copper of the delay line or ground patterns.[17]

In the finished anode each delay line consists of a serpentine strip covering a 100 mm $\times$ 80 mm area. Each of the 160 straight segments of the sperpentine is 100 mm long.

5. Transmission-line measurements

We have performed measurements of the anode to measure its dc parameters and its performance as two independent transmission lines.[3] In Table I, we compare several key performance characteristics[3] for the upper and lower SDLs with and without the bonding and laser ablation.

TABLE I. Delay-line properties with and without bonding/laser ablation processing[a]

	Upper (y)		Lower (x)		
	Free Board	Processed Board	Free Board	Processed Board	Units
Delay time (end-to-end)	107	81	69	66	ns
Transmission	0.16	0.35	0.23	0.37	
Reflection[b]	0.21	0.08	0.13	-0.05	
Rise-time	8.2	6.2	8.5	7.3	ns
v_{eff}	0.74	0.96	1.17	1.22	mm/ns
Cross-talk			< -50 db		
Capacitance	2.7	3.4	1.4	2.1	nF
Z^b	73	60	65	46	Ω

[a]The free boards had 17 μm-thick (nominal) Cu microstrip, while processed board had 50 μm-thick Cu. This mainly affects transmission.

[b]The reflected pulse shows evidence of complex impedence mismatch. Reflectance is not well-defined in this case, and the derived impedances are estimates.

6. Measurement setup

We have tested the detector with light from a Hg-vapor UV lamp (254 nm). A fused-silica optical system[3] focuses an image, at 1:1 magnification, of a single 10-μm diameter pinhole onto the microchannel-plate face. The beam enters the vacuum through a 100-mm diameter fused-silica precision optical flat that is parallel to the microchannel plate. We tested the readout using a bare MCP Z-stack[18] with 10 μm pore diameter and 8 degree bias angle. The anode tested was designed for a 60 mm active area MCP. A less expensive 40 mm diameter active area was used for these tests. The MCP has a very broad global pulse height distribution. The pulse amplitude cuts, used for data in all the analysis presented here, are from $2.8 \times 10^7 e^-$ to $1.4 \times 10^8 e^-$ with the exception of the low pulse-height data presented in section 7.2, which have a range from $6 \times 10^5 e^-$ to $5 \times 10^6 e^-$.

7. Results

In the discussion of the results below, the dimension read out by the lower delay line is denoted x.

7.1. Spatial Linearity

To study the nonlinearities of the SDL we sampled the entire active area using a square grid of 2 mm spacing. The medians of the readout positions exhibit the radial (barrel) distortion that is found in all MCP detectors. This distortion results from the fringing of the electric field in the gap between the MCP and the anode. Application of a radial fit to this distortion leaves residual rms deviations of 42 μm in x and 40 μm in y. The deviations are largely one dimensional, taking the forms $\Delta x(x)$, $\Delta y(x)$, $\Delta x(y)$, and $\Delta y(y)$. Causes for one-dimensional nonlinearities are listed in reference 3. One-dimensional nonlinearities can be corrected very rapidly with small look-up tables. After correcting for $\Delta x(x)$ and $\Delta y(y)$ the rms deviation is 21 μm (x) and 24 μm (y). After correcting additionally for $\Delta y(x)$, and $\Delta x(y)$, the rms deviations are 18 μm for x and 19 μm for y. We discuss causes of nonlinearity in reference 19.

To study nonlinearity at spatial frequencies down to 5 mm^{-1} we used one-dimensional scans with 100 μm between spots through the center of the detector. We analyzed these one-dimensional scans searching for fixed pattern noise at 0.5 mm or 1 mm periods. This would be expected if the anode were incompletely sampling the electron cloud. No such deviations were found.

7.2. Spatial Resolution

The SDL is capable of reading out images with high resolution even with an extremely broad pulse height distribution. We tested the SDL using a MCP with FWHM/peak > 100%. We analyzed data with a dynamic range of 5:1 in pulse amplitude. This requires a software walk correction in which the pulse amplitude range is divided into 10 equal bins (on a linear scale) and the bins are aligned according to the mean position.[3]

We analyzed scans over the central region of the detector, including 85 spots with a total of 4.3×10^4 total events. The spots were combined after first walk correcting each spot independently, as described above, then superposing the spots according to their median positions. The resulting composite point spread function was used to find the FWHM. The resolution is 31 μm in x and 32 μm in y. These values represent the total of all contributions including the incident beam size, the MCP pore spacing, and the readout itself.

The SDL anode and readout electronics limit the SDL resolution in two ways: (1) Voltage noise from the broadband preamplifiers (σ_v) is independent of pulse height. This leads to a signal to noise ratio S/N that is proportional to pulse amplitude, and a resolution contribution that varies inversely with pulse amplitude. (2) The CFD, TAC, and ADC introduce a fixed timing error contribution to the spatial uncertainties that is independent of pulse amplitude. At each amplitude the S/N contribution adds in quadrature to the fixed timing error. Figure 4, which compares the measured x-dimension resolution as a function of pulse amplitude to the predicted contributions, shows that the resolution has minimal dependence on pulse amplitude at high gains, but degrades at low pulse amplitudes as expected from the S/N. The y-dimension is qualitatively similar.

At low pulse amplitude, the contribution of CFD, TAC, and ADC noise is much less than that of preamplifier noise. The predicted contribution of preamplifier noise to (FWHM) spatial uncertainty δx is:

$$\delta x_v = 2.366(\frac{v_{eff}}{2})\sqrt{2}\sigma_t,$$

where the factor of 2.366 is the ratio of FWHM to rms, and the factor of $\sqrt{2}$ is from quadature addition of σ_t from both ends of a delay line. Because the CFD internal delay setting t_d is 5.7 ns, and we have used 39 MHz filters, there is a significant covariance in the noise which reduces its impact on timing. If v is the noise random variable, and α is the constant fraction used in the CFD, we have

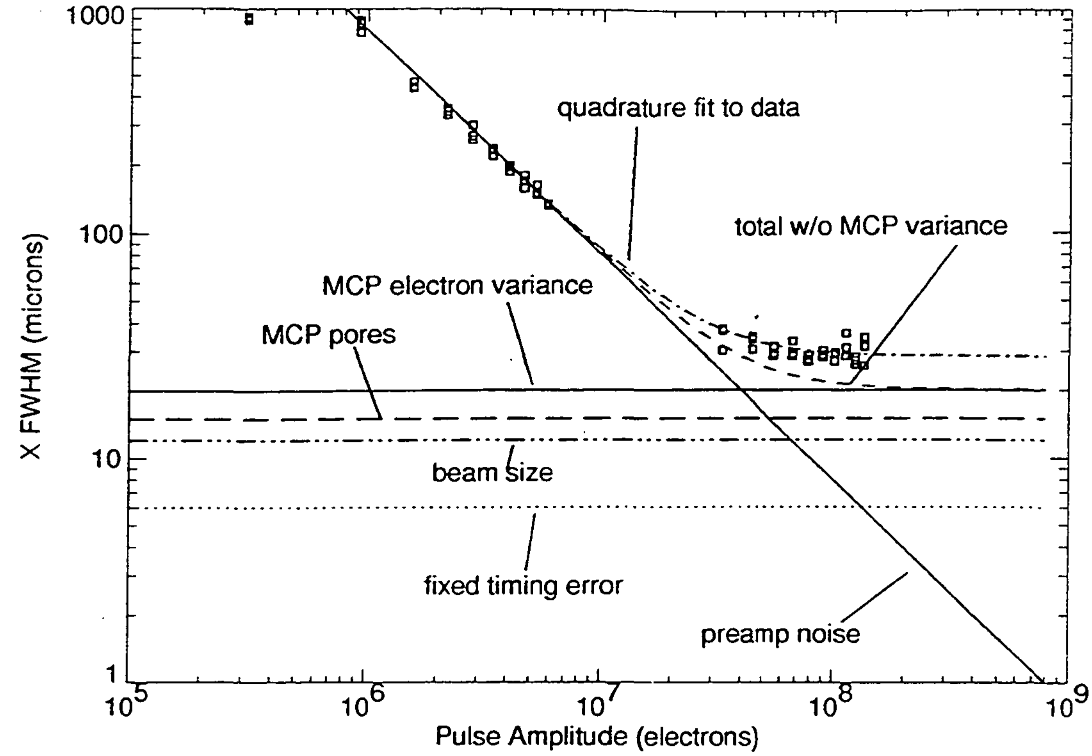

Fig. 4. Spatial resolution vs. pulse amplitude at high and low pulse amplitudes for x. Points show measured resolution. Contributions to the spatial uncertainty include amplifier contribution (best fit to low pulse-height data), UV spot size, MCP pore spacing, fixed timing error, and MCP electron trajectory variance. The solid curve shows the predicted resolution including all contributions except MCP variance, and the dot-dashed curve shows the fit to the data of all contributions, including MCP variance added in quadrature. The difference gives the inferred magnitude of the MCP electron trajectory variance contribution.

$$\sigma_t = \frac{\sqrt{(1+\alpha^2)\sigma_v^2 - 2\alpha\langle v(t)v(t+t_d)\rangle}}{[\dot{V}_{t_0} - \alpha\dot{V}_{t_0+t_d}]}$$

Here, $\langle v(t)v(t+t_d)\rangle$ is the autocovariance function at lag t_d, where t_d, and $\dot{V}_t$ is the time derivative of the wave form evaluated at time t. This equation derives from the details of the analog method[20] by which the CFD determines the time t_0 at which the wave form reaches the fraction α of its peak voltage V_0. $\dot{V}_t$ is roughly proportional to V_0 because the shape of pulses is constant to first order at a given position on the detector. Using measured numbers,[3] we predict $\delta x_v = 52\,\mu\text{m}\,A_7^{-1}$ for the upper delay-line, where A_7 is the pulse amplitude in units of 10^7 electrons. We measured $\delta x_v = 50\,\mu\text{m}\,A_7^{-1}$, in good agreement with the prediction. For the lower delay-line, the slightly higher velocity and lower pulse amplitude give $\delta x_v = 80\mu\text{m}\,A_7^{-1}$, which agrees with the measured $75\mu\text{m}\,A_7^{-1}$.

At high pulse amplitudes, the resolution should be dominated by (1) fixed timing error in the timing electronics, measured to be <10 ps (FWHM) using a test pulser, corresponding to 4.8 μm (x) and 6.1 μm (y); (2) the MCP pore spacing (12 μm center to center); and (3) the width of the focussed spot ($\sim 15\mu m$). This gives a total quadrature contribution of $\simeq 20$ μm. However, at high pulse amplitudes, as Fig. 4

shows, the observed resolution is $\simeq 30\,\mu$m, implying an error in the above sum or a fourth source of spatial uncertainty, contributing $\simeq 20\,\mu$m. We have in fact uncovered a new spatial uncertainty contribution that we have shown is due to event-to-event variance in the trajectory of the electron cloud exiting the MCP[21]. This variance is dependent on the spatial charge distribution exiting the MCP stack. One argument in favor of this conclusion of MCP variance is the fact that using the identical MCP stack at large pulse amplitude, the HDL is observed to have similar resolution in spite of a lower effective velocity and less pulse attenuation[11,12], which would both reduce contributions from the electronics noise. The resolution is roughly constant over the 40 mm area tested at high pulse amplitudes, and typically $< 35\,\mu$m. This is consistent with either MCP electron trajectory variance or fixed timing error. If fixed timing error in the electronics were to blame, the 27% higher velocity of the lower x delay-line would yield resolution 27% worse, while the observed resolution for x is equal or slightly better than y within measurement uncertainty of 3%. This is a second argument in favor of MCP electron trajectory variance.

8. Acknowledgments

We thank Dale Doyle of Rogers Corp. Soladyne Division in San Diego, CA, for his suggestions and oversight during anode fabrication. At the Columbia Astrophysics Laboratory, we thank Irwin Rochwarger for the benefit of his electronics experience and expertise, and Hugh Denning, John Domanski, James Johnson, and Robert Morton for help in fabricating the apparatus. We thank Rick Golish of First Article Services, Inc. in Chandler Arizona for his careful attention to the laser ablation machining of the anode. We also thank Oswald Siegmund for very constructive comments. This work was supported by NASA grants NAG5-642, NAGW-1887, NAGW-2593, NGT-50792 and NGT-50777.

9. References

[1] J. L. Wiza, Nucl. Instr. Meth., **162**, 587 (1979).

[2] G. W. Fraser, X-Ray Detectors in Astronomy, (Cambridge Univ. Press, 1989), Chapter 3.

[3] P.G. Friedman, R.A. Cuza, J.R. Fleischman, C. Martin, and D. Schiminovich, submitted to Rev. Sci. Instrum. (1993).

[4] M. Lampton, O. H. W. Siegmund, and R. Raffanti, Rev. Sci. Instrum., **58**, 2298 (1987).

[5] M. Lampton, O. H. W. Siegmund, and R. Raffanti, IEEE Trans. Nucl. Sci., **37**, 1548 (1990).

[6] O. H. W. Siegmund, private communication (1992).

[7] O. H. W. Siegmund, M. L. Lampton, and R. Raffanti, SPIE Proc., **1159** 476 (1989).

[8] S. E. Sobottka, and M. B. Williams, IEEE Trans. Nucl. Sci., **35**, 348 (1988).

[9] M. B. Williams, S. E. Sobottka, and J. A. Shepherd, Nucl. Instr. Meth., **A302**, 105 (1991).

[10] P.G. Friedman, C. Martin, and A. Rasmussen, SPIE Proc., **1344** 183 (1990).

[11] P. G. Friedman, J. R. Fleischman, and C. Martin, to be published in Proceedings of the 10th Int'l Coll. on UV and X-Ray Spectr. of Astr. and Lab. Plasmas, Feb. 1992, Berkeley, CA), edited by S. Kahn and E. Silver (1993).

[12] P. G. Friedman, R. A. Cuza, J. R. Fleischman, C. Martin, and D. Schiminovich, to be submitted to Rev. Sci. Instrum. (1993).

[13] J. R. Fleischman, P. G. Friedman, C. Martin, and D. Schiminovich *SPIE*, (1993). In this volume.

[14] Rogers Corp., Soladyne Div. San Diego, CA, advised us and manufactured the anode.

[14a] RT/duroid is a trademark of the Rogers Corp., Microwave and Circuit Materials Div. 100 South Roosevelet Ave., Chandler, AZ 85226.

[15] Design Guide for PTFE-Based Circuit Boards, Rogers Corp. Soladyne Division, San Diego, CA. (1989).

[16] The fusion bonding was developed and performed by Rogers Corp.

[17] First Article Services, Inc. in Chandler Arizona cooperated in development of the method used, and performed the laser ablation machining of the anode.

[18] The MCPs were manufactured by Galileo Electro-Optics Corporation.

[19] P. G. Friedman, R. A. Cuza, J. R. Fleischman, C. Martin, and D. Schiminovich, in preparation (1993).

[20] Instruction manual for TC 455 Quad CF Discriminator, Tennelec/Nucleus Inc., Oak Ridge, TN (1983), p.10.

[21] P. G. Friedman, R. A. Cuza, J. R. Fleischman, C. Martin, and D. Schiminovich, in preparation (1993).

APPENDIX C

COLUMBIA UNIVERSITY

INVENTION REPORT AND RECORD

INVENTOR(S):

Name Peter Gray Friedman — Position Associate Research Scientist

University Address 1013 Pupin Hall — Telephone (212) 854-8081

Name Christopher Martin — Position Associate Professor of Physics

University Address 1012 Pupin Hall — Telephone (212) 854-7490

(Include additional names and addresses on a separate sheet.)

DESCRIPTIVE TITLE OF INVENTION

Crossed serpentine delay-line anode for high resolution, two-dimensional, digital readout of images from microchannel-plate detectors of light or radiation.

GRANT/CONTACT (If any):

Sponsor NASA — Award Number NAG 5-642, NAGW-1887, NAGW-2593

Principal Investigator: Christopher Martin

LAB/DEPARTMENT WHERE DEVELOPED:

UV Lab of the Columbia Astrophysics Laboratory

DESCRIPTION OF INVENTION:

1. State, as fully as possible, what the invention is, including: materials or components used; operative and preferred ranges of process parameters and concentrations of chemical compounds; and foreseeable uses of the invention.

The serpentine delay-line anode is a multilayer, slotted, printed circuit board of novel architecture, made from copper and dielectric material, and bonded to a metal plate. The anode converts a burst of electrons, emitted by microchannel plate, into voltage pulses with timing that permits the determination of the position of incident photons or particles. The anode can be used for all available sizes of microchannel plates, at event rates of up to $\sim 10^6$/sec. The anode provides several thousand pixels in both dimensions of the image. Applications include space- and ground-based astronomy, X-ray crystallography, mass spectrometry, surface analysis, detection of missle launches in reconnaissance satellites, and medical imaging.

B. **Records Supporting Invention: Identify records which establish dates of conception and reduction to practice, including identity of person who prepared record and its present location. Attach copies if possible. Note additional supporting evidence. If the invention or a significant aspect of the invention is not supported by written records, briefly describe how the date of invention can be established and identify earliest written record.**

Laboratory logbooks record tests of components and functioning detector. First entry: UV Lab logbook VII, p. 58, dated 24 June 1992.

First request for quote (RFQ) is undated. Revision dated 3/22/92.

Hand written notes by Friedman and Martin, of phone conversations with manufacturer.

Computer files of early drafts of drawing for RFQ may be earliest record.

It might be possible to find hand written notes of discussions between Friedman and Martin which would be the earliest record.

C. **Fill in the following dates:**

1. **Conception** January or February 1992
2. **First disclosure to another** Judith Fleischman, January or February 1992
3. **First written record** See B above.
4. **First experiment demonstrating the invention** 6/24/92 anode components; Dec. 92 or Jan. 93 functioning detector

D. **This invention is a(n):** ____ **Process** ____ **Chemical compound** X **electronic circuit** ____ **mixture of chemical compounds** X **apparatus** ____ **therapeutic method** X **other (describe)** ____

E. **This invention is useful as** an anode for position sensitive two-dimensional readout of microchannel-plate detectors.

F. **The problem which this invention solves is** the digital readout of images with several thousand pixels in both dimensions, with event rates up to $\sim 10^6$/sec., by a device that is robust for space launch, simple to operate, inexpensive, and can be mass-produced.

G. **The closest prior art is** 1) S.E. Sobbottka and M.E. Williams, IEEE Trans. Nucl. Sci. 35, 348 (1988) -- wire-wound two dimensional crossed helical delay line anode.
2) M. Lampton et al., IEEE Trans. Nucl. Sci., 37, 1548 (1990) -- single layer printed circuit board anode, delay-line method used for only one dimension.

H. This invention differs from the closest prior art in that it has neither wound wires (1), nor several times fewer pixels and wasted space in one readout dimension (2).

I. This invention provides the following advantages simplicity, low cost, robustness, many pixels in both image dimensions, high throughput rate, low operating power, and can be mass-produced.

J. Has the invention or any product derived therefrom been:

1. Described in a printed publication? No Date ________

2. Described in an oral presentation? Yes Date 4/13/93

3. Sold, offered for sale, or used in public? No Date ________

4. Are any of the above (1-3) contemplated in the near future and, if so, when? Journal article submitted and being revised, oral presentation 7/11/93

5. If the answer to any of 1 through 4 is yes, provide detailed information, including copies of manuscripts, published articles, abstracts, etc.

K. Is the invention embodied in software? No

If so,

1. Does the software include any novel algorithms, formulas or novel applications of known algorithms or formulas? If so, please identify them and describe their function.

____

____

2. Does the invention include a database? ________

3. If there is a database, is the database structure novel? If it is, please describe how it is novel. ________

____

____

4. Does the invention include any novel features relating to display screen presentation? If so, please identify these novel features. ________

____

____

CONTACT/AGREEMENTS WITH COMMERCIAL CONCERNS (Include name of person contacted and copies of pertinent agreements)

Contact + P.O. - Rogers Soladyne Div.: Dale Doyle

Contact + subcontract through Rogers - First Article, Inc.: Rick Goulish

I/We submit this Invention Report and Record pursuant to Columbia's Statement of Policy on Proprietary Rights in the Intellectual Products of Faculty Activity, adopted by the Trustees of the University, on June 5, 1989. If, pursuant to this Policy, the University determines to seek patent or other appropriate protection for the invention described herein, I/We shall cooperate with the University in its efforts to do so and shall sign such documents as may be required for this purpose, including an assignment of the invention to the University. I/We understand that the University will adhere to the terms of the attached Statement of Policy, and will divide any proceeds from the invention according to those terms. I/We also understand that if the University decides not to seek protection for the invention, it will, upon request and where permitted by Federal law governing inventions made with Federal funding, release its rights in the invention to me/us.

Inventor (s) ______________________ Date: ______________________

______________________ Date: ______________________

______________________ Date: ______________________

______________________ Date: ______________________

Receipt is hereby acknowledged:

______________________________ Date: ______________________

Office of Science and Technology Development

Columbia University in the City of New York | *New York, N.Y. 10027*

OFFICE OF SCIENCE AND TECHNOLOGY DEVELOPMENT

411 Low Memorial Library
(212) 854-8444
FAX (212) 854-8463

January 6, 1994

Ref.: "Serpentine Delay Lines.." Inv. Report M93-033xx

Dear Drs. Peter G. Friedman
Christopher Martin

Pursuant to Paragraph F of the University's Statement of Policy on Proprietary Rights in the Intellectual Products of Faculty Activity, dated June 5, 1989, I am writing to advise you that the University does not intend to participate in seeking patent protection for the above-referenced invention, described in the Invention Report submitted to this office, dated June 26, 1993. After examining the potential commercial applications for this invention, we have concluded that they are too limited to warrant the considerable costs of patent filing, prosecution, and maintenance.

If you would like to pursue patent protection at your own expense, please call this office so that we can discuss how the University, consistent with applicable Federal law, might effect a transfer of its rights in the invention to you.

Sincerely yours,

Jack M. Granowitz,
Director

cc: Beth H. Israel
Fred H. Kant